frontiers in Physics

ORIGINAL RESEARCH
published: 04 October 2021
doi: 10.3389/fphy.2021.737205

Multi-Chromophore Dyes for Improving Light Stability of Electro-Fluidic Displays

Yong Deng[1], *Dechao Ye*[1], *Yuanyuan Guo*[2], *Guofu Zhou*[1,2] *and Hongwei Jiang*[2]*

[1]Academy of Shenzhen Guohua Optoelectronics, Shenzhen, China, [2]South China Academy of Advanced Optoelectronics, South China Normal University, Guangzhou, China

Electro-fluidic display (EFD) is a new reflective display based on electrowetting phenomenon which is applied to the outdoor billboard. Organic dyes are the most important materials for the color gamut and reliability of the EFD devices, which are always synthesized based on mono-chromophore dye in previous work. In this paper, we report our research on azopyrazolone as the chromophore to construct a polychromic macromolecular dye system. The light stability and photo-electric properties of these new dyes are researched detailed. It is found that the light stability of multi-chromophore dyes and backflow properties are much better than corresponding mono-chromophore dye.

Keywords: colored oil, photo-stability, azo pyrazolone dyes, electro-fluidic display, multi-chromosome dyes

OPEN ACCESS

Edited by:
Feng Chi,
University of Electronic Science and Technology of China, China

Reviewed by:
Hui Li,
Shenzhen University, China
Jingjing Yang,
Nanjing Xiaozhuang University, China

***Correspondence:**
Hongwei Jiang
hongwei.jiang0822@gmail.com

Specialty section:
This article was submitted to Optics and Photonics, a section of the journal Frontiers in Physics

Received: *06 July 2021*
Accepted: *21 September 2021*
Published: *04 October 2021*

Citation:
Deng Y, Ye D, Guo Y, Zhou G and Jiang H (2021) Multi-Chromophore Dyes for Improving Light Stability of Electro-Fluidic Displays. Front. Phys. 9:737205. doi: 10.3389/fphy.2021.737205

INTRODUCTION

Recently, electro-fluidic display as an emerging display technology has received widespread attention [1–4]. It has many advantages such as fast response time and full-color compared to electrophoretic display [5–7]. In electro-fluidic devices, transparent polar liquids play the role of changing wettability on solid surfaces to realize various applications. The contact angle of polar liquid on solid surface is determined by Young's equation as shown in **Eq. 1**.

$$\cos\theta_0 = \left(\gamma_{sg} - \gamma_{sl}\right)/\gamma_{\mathrm{lg}} \tag{1}$$

where θ_0 is the initial contact angle of liquid on solid, γ_{sg} is surface tension of solid-gas, γ_{sl} is surface tension of solid-liquid, while γ_{lg} is surface tension of liquid-gas. θ_0 is a constant, which only depends on the physical properties of liquid and solid.

When a voltage is applied across the polar liquid and solid, the contact angle of polar liquid on solid surface will be changed, and it obeys Young-Lippmann equation, as shown in **Eq. 2**.

$$\cos\theta_V = \cos\theta_0 + \varepsilon_0\varepsilon_r V^2/2d \cdot \gamma_{\mathrm{lg}} \tag{2}$$

where θ_V is contact angle with a voltage applied, ε_0 is dielectric constant in vacuum, ε_r is the effective dielectric constant of dielectric layer, V is electromotive force applied between solid surface and polar liquid, d is the thickness of dielectric layer.

Colored oil, another critical material in electrowetting display, is not miscible with polar liquids. The movement of polar liquid promotes the contraction and spread of ink to achieve the display purpose. An unbalance force ΔF can be formed in the polar liquid with a voltage applied, and the phenomenon is that the liquid has an advancing angle and a receding angle. The unbalance force ΔF is the initial force that drives the movement of polar liquid, and its magnitude of force follows **Eq. 3**.

$$\Delta F = \gamma(\theta_1 - \theta_2) = \frac{1}{2}CV^2 = \frac{1}{2}\frac{\varepsilon_r \varepsilon_0 A}{d}V^2 \quad (3)$$

Colored oils are so important in electrowetting display that lots of special dyes have been disclosed in previous research, such as the designation of anthraquinone dyes [8, 9], azo dyes [10–14], dipyrrole methane metal dyes [15], and pigment dispersion [16, 17]. However, all the dyes are mono-chromophore structure, which cannot avoid the backflow caused by dye's polarization.

The tendency of oil to flow back into pixel at a constant voltage is called "backflow". The reduction of oil contraction affects the pixel aperture for "backflow" oil, which has an impact on the power consumption of the display. Since a static reading mode is operated for an EFD display, low "backflow" oil will lead to the decrease of refresh rate for display. Thus, the power consumption can be reduced because of its scaling with the refresh rate. Studies have shown that the addition of polar dye molecules has a negative effect on ink reflow [18, 19]. Due to their polarities, the dye molecules are oriented under an external electric field, and the affinity between the oil and the hydrophobic layer increases. Polarized dye molecules also tend to cause external charges and penetrate at the three-phase contact line of the ink-water-insulation layer, which eventually caused the electrostatic force F.

Moreover, a large number of experiments have shown that the light stability of dye molecules is depended on their molecular structure. The greater aggregation is, the better the light stability of dyes have. When the same amount of dye molecular exposed to air, moisture and sunlight, the smaller surface area of the molecule is, the lower probability of dye molecule being oxidized by light. Conversely, when the dye is dissolved in a mono-disperse state, the surface area of the molecule is much higher than aggregation state, thus the chance of photo-oxidation or photo-reduction reaction is great. G. Baxter research shows that when the dye molecules are present in a highly disperse state, the photo-fading reaction is an apparent first-order reaction, while the photo-fading reaction of the dye molecules in the aggregation state is an apparent 0-order reaction [20]. It was also found that water-insoluble dyes have stronger internal molecular forces in the aggregation state, which makes it easier to transfer energy, and connect dye molecules through bridges to increase the degree of dye aggregation and reduce the overall molecular weight.

In this paper, azopyrazolone dye is used as the chromophoric matrix to construct a multi-chromophore macromolecular dye system, using binding effect of the bridge group in space to reduce the dipole moment of the entire molecule, thereby reducing the backflow effect of oils under external electric field. The polychromatic azopyrazolone-type molecules have an increased degree of chromophore aggregation, which may strengthen the chromophore's bridge-based molecular skeleton energy transfer channel, induction effect, and covalent bond action. Therefore, the design of this type of dye has high solubility, absorption coefficient and light stability.

EXPERIMENTAL

Materials

Chemicals are purchased analytically pure and used without further purification. Indium Tin Oxide, SU-8 3,005 photoresist, AF Teflon® 1,600X were purchased and used in industrial grade.

Electro-Fluidic Display Oil Formulation and Device Fabrication

Dyes and solvents were calculated and weighted in a cell, dissolved, and filtrated with a 0.2 μm filtrator. The filtration was collected as EFD oil and used to formulate EFD device followed by our previous process [21].

Dye Synthesis and Characterization

The structures of three designed dyes were shown in **Figure 1**. D-1: 1.27 g (121 g/mol, 0.01 mol) 4-aminophenylethane was dissolved in 20 ml water in a three-necked flask with agitation, and the solution was heated to 80°C until it dissolved completely. Then, hydrochloric acid (4.2 ml, 12 mol/L) was added dropwisely and the solution was quickly cooled down to 0–5°C. Then 1.04 g of sodium nitrite (1.5 times, 69 g/mol) was added at one time, the solution was continuously stirred for 2 h. The temperature of the reaction system was kept at 0–5°C. The Ehrlich reagent was used to detect the end of the diazotization reaction. After that, a certain amount of urea is added to remove unreacted sodium nitrite. 4.56 g (294 g/mol, 0.02 mol) of 3- (1-ethylpentyl) -1- (1-ethylhexyl) -2-pyrazolin-5-ol and sodium carbonate were solute in ethanol. The diazo salt solution prepared above was added into the solution dropwisely in 2 h. After that, the solution was poured into 100 ml water, and 30 ml ethyl acetate and petroleum ether solution (1:10, v/v) was used to extract the yellow dye. The organic layer was collected and evaporated to get 3.51 g crude product D-1. The crude D-1 was purified by flash chromatography on silica gel (eluting agent: petroleum ether and ethyl acetate). Characterization: D-1; yield: 82.9%; λ (max) = 420 nm (in decane); ε = 11,730 L mol^{-1}·cm^{-1}. IR (KBr, cm^{-1}): 3,071.2(Ar-H); 2,963.1(-CH_3), 2,928.1(-CH_2-), 2,857.2(-CH_3); 1,642.2(-C=O); 1,581.8(Ar); 1,551.2(Ar-H), 1,524.8(Ar),1,459.9(-CH-),1,378.2(-CH_3), 1,254.1(C-N-C); ^{1}H NMR (400 MHz, $CDCl_3$): 13.796(s, 1H), 8.442(s, 1H), 7.639(m, 6H), 7.610(m, 2H), 7.232(m, 2H), 7.256(m, 2H), 4.580(m, 2H), 3.739(m, 2H), 2.698–2.559(m, 1H), 1.550–1.521(m, 4H), 1.289–1.233(m,12H), 0.899–0.7599(m,12H); ^{13}C NMR (400 MHz, $CDCl_3$): 182.11, 146.560, 134.570, 131.840, 126.030, 123.660, 109.670, 45.990, 39.470, 31.280, 29.040, 24.530, 23.030, 14.120, 10.990; MS (MALDI-TOF) (DIF) M/Z (%): 427.3.

Intermediate: 1.27 g (137 g/mol, 0.01 mol) 4-aminophenethyl alcohol was dissolved in 20 ml water in a three-necked flask with agitation, and the solution was heated to 80°C until it dissolved completely. Then, hydrochloric acid (4.2 ml, 12 mol/L) was added dropwisely and the solution was quickly cooled down to 0–5°C. 1.04 g (0.015 mol, 69 g/mol) of sodium nitrite was added at one time, the reaction was last for 2 h. The temperature of the reaction system was kept at 0–5°C. The Ehrlich reagent was used to detect the end of the diazotization reaction. A certain amount of urea is added to remove unreacted sodium nitrite. 4.56 g (294 g/mol, 0.02 mol) of 3- (1-ethylpentyl) -1- (1-ethylhexyl) -2-pyrazolin-5-ol and sodium carbonate were solute in ethanol. The diazo salt

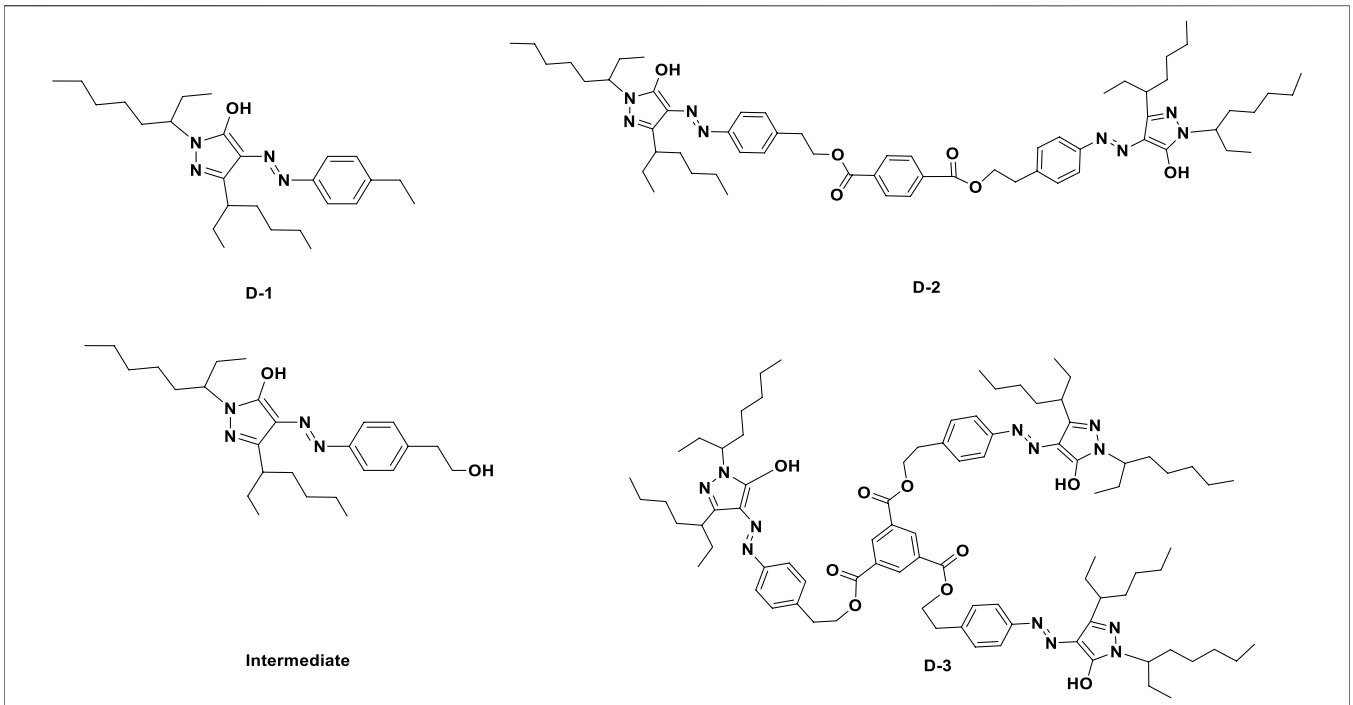

FIGURE 1 | Molecular structures of the Intermediate and three synthesized dyes.

prepared above was added into the solution dropwisely in 2 h. After that, the solution was poured into 100 ml water, and 30 ml ethyl acetate and petroleum ether solution (1:10, v/v) was used to extract the yellow dye. The organic layer was collected and evaporated to get 3.60 g crude product. The crude Intermediate was purified by flash chromatography on silica gel (eluting agent: petroleum ether and ethyl acetate); yield: 81.9%; λ (max) = 420 nm (in decane); IR (KBr, cm^{-1}): 3,061.3 (Ar-H), 2,951.3(-CH_3), 2,921.1(-CH_2–), 2,880.1(-CH_3); 1,642.9(-C=O), 1,582.8(Ar); 1,555.2(Ar-H), 1,521.2(Ar); 1,458.9 (-CH-); 1,379.1(-CH_3); 1,257.3 (C-N-C); 817.8. ^{1}H NMR (400 MHz, $CDCl_3$): 13.781(s, 1H), 8.421(s, 1H), 7.76(m, 6H), 7.622(m, 2H), 7.262(m, 2H), 7.267(m, 2H), 4.555(m, 2H), 3.555(m, 2H), 2.670–2.551(m, 1H), 1.548–1.526(m, 4H), 1.283–1.245(m, 12H), 0.891–0.761(m, 12H); ^{13}C NMR (400 MHz, $CDCl_3$): 190.090, 144.460, 134.480, 132.440, 127.480, 124.640, 110.140, 44.490, 38.470, 32.480, 29.920, 24.620, 22.520, 15.230, 11.890; MS (MALDI-TOF) (DIF)M/Z (%): 443.3.

D-2: 0.58 g Intermediate was dissolved in 20 ml n-decane, then 0.1 g (0.30 mmol, 234 g/mol) 1,4-phthaloyl chloride and 4.2 ml (91 g/mol, 0.2 mol) triethylamine was added dropwisely into the reaction solution. The temperature was raised to 50°C. TLC was used to monitor the termination of reaction. After the reaction was completed, the solution was cooled down, and poured into 100 ml water. 50 ml petroleum ether was used to extract the product three times, and the oil layers were collected and rotary evaporated. Then the crude product D-2 was column purified with 1: 120 of n-hexane and petroleum ether mixture as eluent. Compound D-2 was obtained as yellow dye with yield of 82.0%. λ (max) = 420 nm (in decane); ε = 16,119 L mol^{-1} cm^{-1}. IR (KBr, cm^{-1}): 3,061.2(Ar-H), 2,962.5(-CH_3), 2,921.5(-CH_2–), 2,859.5(-CH_3), 1,645.3(-C=O), 1,581.3(Ar), 1,555.1(Ar), 1,521.2(Ar), 1,458.9(-CH-), 1,378.2(-CH_3), 1,257.8(C-N-C); ^{1}H NMR (400 MHz, $CDCl_3$): 12.998 (s, 2H)8.420(s, 2H), 7.389(m, 3H), 7.253 (m, 2H), 4.590(m, 2H), 3.541(m, 2H), 2.669–2.551(m, 2H), 1.536–1.518(m, 4H), 1.287–1.253(m, 24H), 0.901–0.753(m, 24H). ^{13}C NMR (400 MHz, $CDCl_3$): 181.110, 145.560, 139.130, 134.370, 131.240, 126.230, 123.260, 114.220, 109.620, 45.920, 39.420, 31.220, 29.030, 24.230, 23.230, 14.130, 10.890; MS (MALDI-TOF) (DIF)M/Z (%): 1,015.8.

D-3: 0.58 g Intermediate was dissolved in n-decane, 0.1 g (0.30 mmol, 234 g/mol) 1,3,5-trisyl chloride and 4.2 ml (91 g/mol, 0.2 mol) triethylamine was added dropwisely in the reaction solution. The temperature was raised to 50°C. TLC was used to monitor the termination of reaction. After the reaction was completed, the solution was cooled down, and poured into 100 ml water. 50 ml petroleum ether was used to extract the product three times, and the oil layers were collected and rotary evaporated. Then the crude product D-3 was column purified with 1: 120 of n-hexane and petroleum ether mixture as eluent. D-3 was obtained as yellow dye with yield of 85.0%. λ (max) = 420 nm (in decane); ε = 49,710 L mol^{-1} cm^{-1}. IR (KBr, cm^{-1}): 3,062.7(Ar-H), 2,962.7(-CH_3), 2,922.4(-CH_2-), 2,882.3(-CH_3), 1,642.7(-C=O), 1,582.7(Ar); 1,552.1(Ar); 1,523.9(Ar); 1,453.8(-CH-); 1,379.2(-CH3); 1,257.2(C-N-C); 816.7. ^{1}H NMR (400 MHz, $CDCl_3$): 13.555 (s, 3H)8.834(s,3H), 7.349–7.332(m, 12H), 4.581–4.573(m, 6H), 3.715–3.684(m, 3H), 3.143–3.137(m, 6H), 2.608–2.577(m, 3H), 1.70(m, 6H), 1.541–1.519(m, 12H), 1.519(m, 6H), 1.371–1.248(m, 33H), 0.891–0.879(m, 27H). ^{13}C NMR (400 MHz, $CDCl_3$): 181.110, 146.460, 133.570, 132.840,

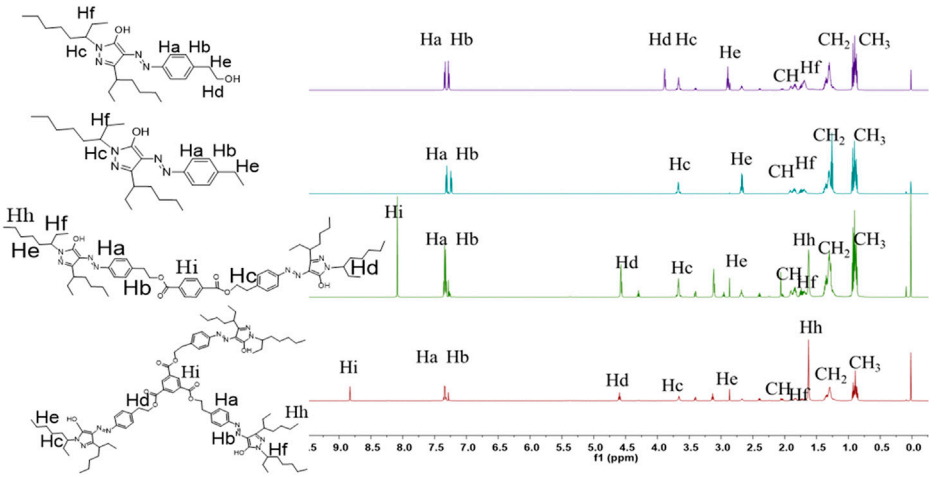

FIGURE 2 | ^{1}H NMR spectra of three synthesized dyes and Intermediate.

125.030, 123.560, 114.590, 109.570, 45.590, 39.450, 31.250, 29.050, 24.550, 23.050, 14.150, 10.590; MS (MALDI-TOF) (DIF)M/Z (%): 1,483.5.

RESULTS AND DISCUSSION

The ^{1}H NMR spectra for the target molecules recorded in $CDCl_3$ are shown in **Figure 2**. The structures of dyes were confirmed by the presence of four distinct downfield signals characteristic of the aromatic rings. For D-1 and Intermediate, the structure of pyrazoline ring was confirmed by the presence of four distinct downfield signals ("Ha", "Hb"). The "Ha" and "Hb" protons of D-1 and Intermediate exhibited two doublets between 7.27 ppm and 7.58 ppm. For the substituents in the N-position, these two dyes displayed one common multiple peak "Hc" between 3.50 and 4.00 ppm, corresponding to the methene protons adjacent to the imide group. The "Hd" protons appeared as a singlet between 3.88 and 4.00 ppm. For the other pyrazolone dyes D-2/3, the "Ha" and "Hb" protons of D-2/3 exhibited two doublets between 7.50 ppm and 7.25 ppm. The "Hi", protons of D-2 exhibited one singlet at 8.23 ppm. The "Hi", protons of D-3 exhibited one singlet at 8.95 ppm. Two dyes: D-2/3, displayed one common multiple peak "Hc" and "Hd" at 4.60 and 3.78 ppm corresponding to the methene protons adjacent to the imide group and O atom. Moreover, the common multiple peak "Hf" of those four molecules represented the protons on the methyl group, and the "CH" protons existed between 0.78 and 0.92 equivalent to the number of protons which were obtained. The chemical values confirmed the structural correctness of the four molecules.

Absorption Properties of Dyes

As can be seen in **Figure 3**, the uv-visible absorption spectra and data of all the dyes were recorded in decane. It is found that the maximum wavelength numbers (λ_{max}) of three dyes D-1/3 are all at 420 nm, showing a same color of yellow. The maximum wavelengths are independent with the number of chromophoric matrix. The molar extinction coefficients of the three dyes are 11,730, 38,470 and 49,710 L mol^{-1}·cm^{-1} for D-1, D-2 and D-3, respectively. And we can see from **Figure 3B,** as the number of chromophore increase, the molar extinction coefficient of the dyes increase.

Electrowetting Properties

The contact angle of DI water droplet on AF (amorphous fluoropolymers) surface in different ambient oil was characterized by varying the applied voltage between the Pt electrode and the substrate electrode in the range of −40 to 40 V at a ramp speed of 1V/1s to demonstrate the potential of EW-based tensiometry. The initial contact angle of DI-water droplet on the AF surface was at ~145° in D-1 oil. The contact angle gradually decreased from ~145° to ~105° as the applied voltage was changed from 0 to ±40 V. The initial contact angle of DI-water droplet on AF surface was at ~154° in D-2 oil. The contact angle gradually decreased from ~154° to ~113° as the same applied voltage change. The initial contact angle of DI-water droplet on AF surface was at ~156° in D-3 oil. The contact angle gradually decreased from ~156° to ~123°. The data shown in **Figure 4** are collected over two cycles, during which the voltage is slowly ramped up and down. The dc results conclusively showed that a strong and reversible electrowetting response can be achieved in the three different kinds of oil.

Backflow Effect of Oils

Synthesized dyes were designed to analyze the effect of dye molecular structure on electrowetting backflow effect. As D-2 has low solubility in decane, only D-1 and D-3 were tested in devices. According to the experimental data shown in **Figure 5**, the backflow time of D-1 device is 150 s, and the backflow time of D-3 device is 250 s. Comparing the backflow time of the D-1 and D-3 devices, it can be clearly seen that D-3 device has longer backflow time, which can be attributed to the smaller dipole moment of D-3. As the arrangement direction of three chromophores in D-3 is non-uniformity, thus the dipole

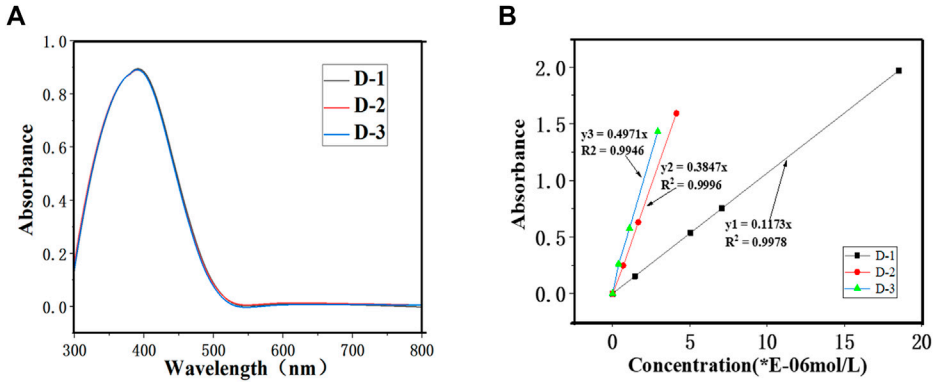

FIGURE 3 | (A) UV-visible absorption spectrum of three dyes **(B)** Working curve of three dyes.

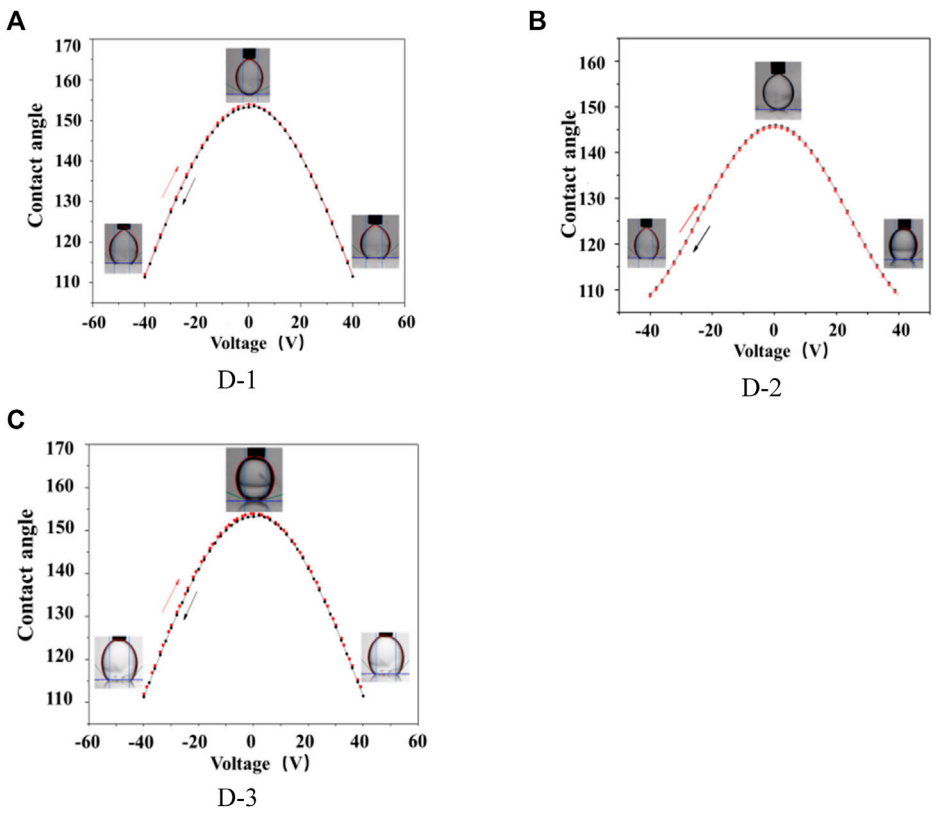

FIGURE 4 | Contact angle of water in oils on AF layer as a function of DC voltage. **(A)** D-1; **(B)**: D-2; **(C)**: D-3; Solvent: decane.

moment of whole dye D-3 will be partially or completely cancelled out.

Photoelectric Response Properties of Dyes

The photoelectric response properties of D-1/3 dyes were demonstrated by measuring the capacitance of the EFD cell under different voltage. The results could be seen in **Figure 6**. As the voltage raise from 0 to 40 V, we can see that the capacitance of the cell has an abrupt change point at 26 V, showing that the oil begins to break up and shrink at 26 V, which is called the threshold voltage. When the voltage decreased from 40 to 0 V, we can see that the capacitance of the cell decreased gradually as expected, which didn't suffer an abrupt change. The CA hesterisis and existing of oil film rupture corresponded threshold voltage caused the asymmetry of the C–V curves in ON and OFF process. D-3

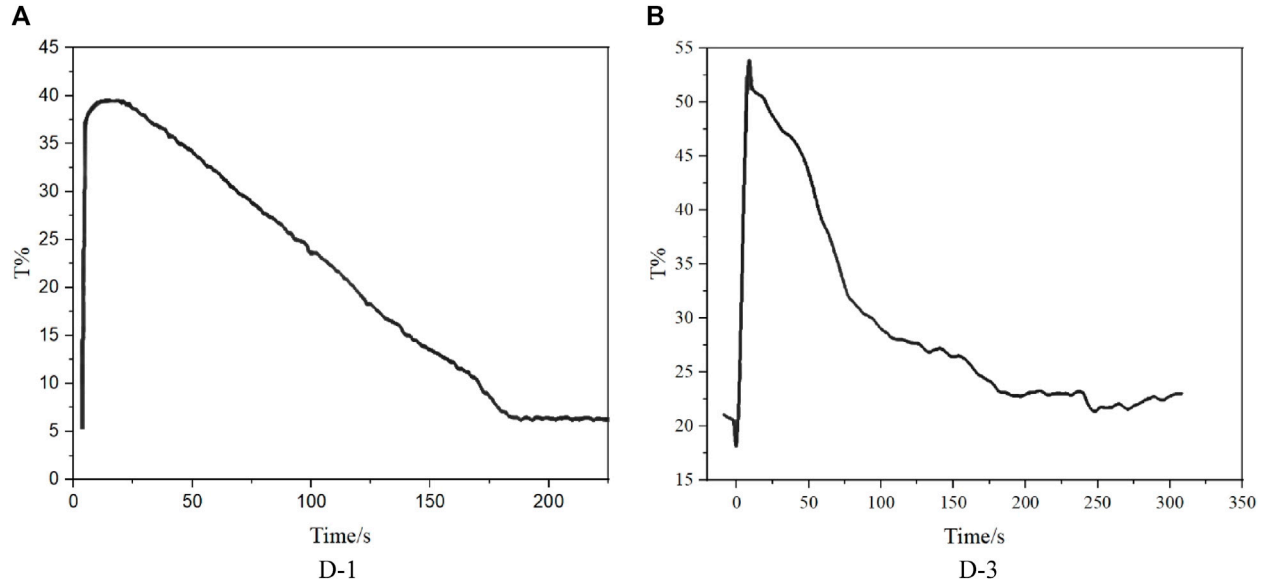

FIGURE 5 | Backflow time of electrowetting display devices formulated by Dyes D-1/3. **(A)**: D-1; **(B)**: D-3.

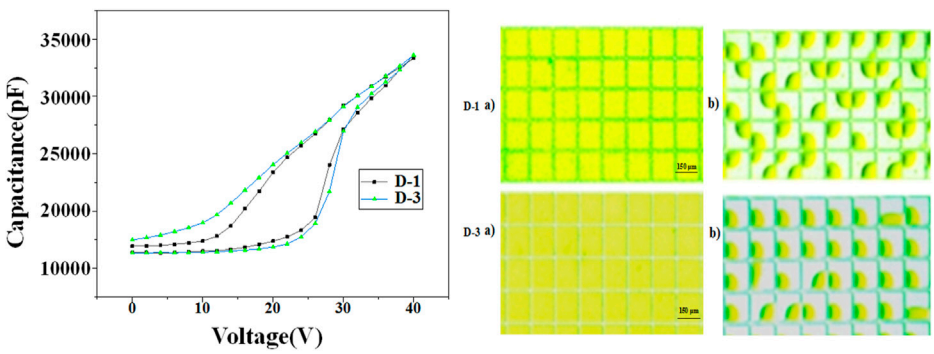

FIGURE 6 | Photoelectric response properties of dyes D-1/3.

has more smoothly curve when the voltage decrease, that's because D-3 has lower electric susceptibiltiy than D-1, the retracted oil drop is more stable at certain voltage. The photos of EFD device at ON and OFF states were recorded, and the aperture ratios were calculated in photoshop software. The aperture ratio of D-1 and D-3 could reach as high as 68.5 and 75% respectively.

Light-Stability Research of Dyes

As researched by G. Baxter and Shufen Zhang, the dye molecules under aggregation state have stronger internal molecular force, which makes it easier to transfer energy, thus the aggregation have much better light stability. The light stability comparison of multi-chromophore dye and corresponding mono-chromophore dye were researched. The test was carried under accelerated xenon lamp for 100 h at 45°C, which can translate to several years of normal conditions [22].

The color coordinates of colored EFD cell formulated by D-1 and D-3 were tested, the results were showed in (x, y) in CIE1931 color space. The color deviation ΔE were calculated from the deviation of l, a, b value. The results could be seen in **Figure 7** and **Table 1**. For D-1, as the irradiation time increased, color coordinates (x, y) of EFD panel were changed. The color coordinate x increased from 0.426 to 0.440, while the color coordinate y increased from 0.416 to 0.432, showing that the color changed from bright yellow to light yellow. The ΔE of D-1 was found to be as high as 2.680 after 100 h of irradiation. For the D-3, the color coordinate x increased from 0.464 to 0.466, while the color coordinate y did not change. The ΔE of D-3 was 1.200, showing a very

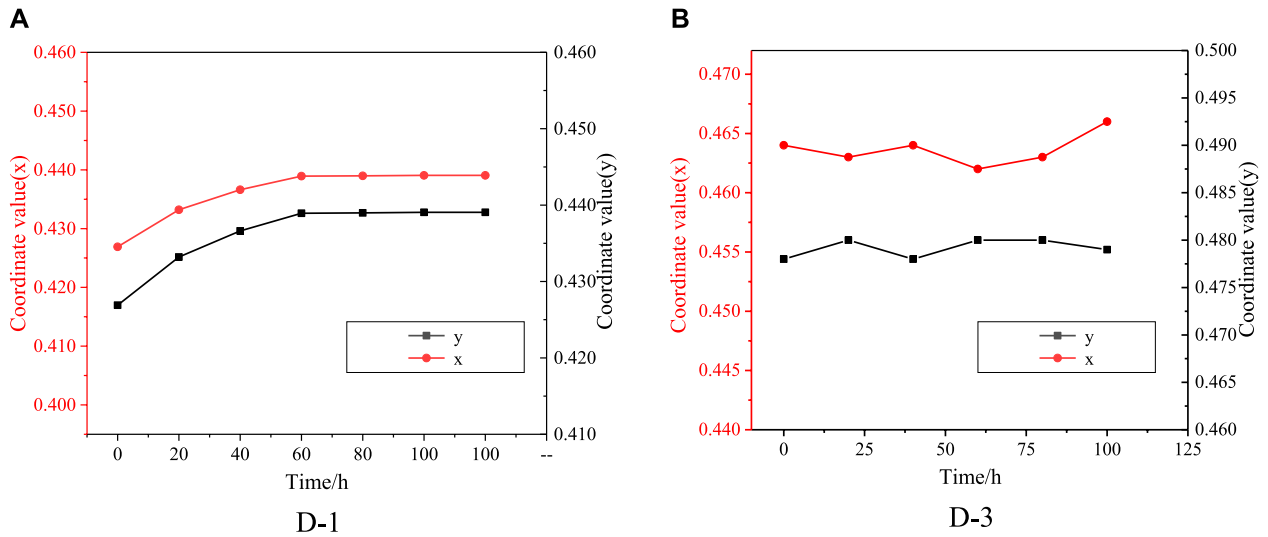

FIGURE 7 | Variation of color coordinates (x, y) of oils in CIE1931 color space (Irradiation condition: 0.55 W/m^2 (340 nm); Temperature 45°C); **(A)**: D-1; **(B)**: D-3.

TABLE 1 | Color change (ΔE) of two formulated dyes before and after accelerated irradiation.

Dye	Before irradiation			After irradiation			ΔE
	L	A	b	L	A	b	
D-1	246.500	−8.720	182.640	244.030	−7.680	182.670	2.680
D-3	239.400	14.000	210.500	238.300	14.400	210.300	1.200

(Irradiation condition: 0.55 W/m^2 (340 nm); Irradiation time: 100 h; Temperature 45°C).

small color change which can hardly be distinguished by the naked eye after 100 h irradiation. These performances are highly relevant to their structure stability.

CONCLUSION

In summary, we have constructed a multi-chromophore macromolecular dye system and synthesized three EFD oil materials based on azo pyrazolone dyes. The absorption, electrical-optical response, and light-stability of these dyes were researched in detail. The three-chromophore dye D-3 has higher aggregation and lower polarity than mono-chromophore dye D-1, thus it has low backflow effect and good light-stability. The research showed that low polarity and high degree of dye aggregation can highly increase the light-stability property and decrease the backflow of EFD oil.

DATA AVAILABILITY STATEMENT

The original contributions presented in the study are included in the article/Supplementary Material, further inquiries can be directed to the corresponding author.

AUTHOR CONTRIBUTIONS

HJ and YD conceived the idea; YD conducted the analyses; HJ, DY, YG, and GZ provided the data; all authors contributed to the writing and revisions.

FUNDING

This work was supported by National Natural Science Foundation of China (22,008,156), Program for Guangdong Innovative and Enterpreneurial Teams (No. 2019BT02C241), Science and Technology Program of Guangzhou (No. 2019050001, No. 201904020007), Program for Chang Jiang Scholars and Innovative Research Teams in Universities (No. IRT_17R40), National Natural Science Foundation of Guangdong, China (2018A0303130059), Guangdong Provincial Key Laboratory of Optical Information Materials and Technology (Grant No. 2017B030301007), Guangzhou Key Laboratory of Electronic Paper Displays Materials and Devices (201,705,030,007), MOE International Laboratory for Optical Information Technologies and the 111 Project.

REFERENCES

1. Hayes RA, and Feenstra BJ. Video-speed Electronic Paper Based on Electrowetting. *Nature* (2003) 425(6956):383–5. doi:10.1038/nature01988
2. Tang B, Groenewold J, Zhou M, Hayes RA, and Zhou G. Interfacial Electrofluidics in Confined Systems. *Sci Rep* (2016) 6(1):26593. doi:10.1038/srep26593
3. Berge B, and Peseux J. Variable Focal Lens Controlled by an External Voltage: An Application of Electrowetting. *The Eur Phys J E.* (2000) 3(2):159–63. doi:10.1007/s101890070029
4. Riahi M, Brakke KA, Alizadeh E, and Shahroosvand H. Fabrication and Characterization of an Electrowetting Display Based on the Wetting-Dewetting in a Cubic Structure. *Optik* (2016) 127(5):2703–7. doi:10.1016/j.ijleo.2015.11.205

5. Sung Kwon Cho SK, Hyejin Moon H, and Chang-Jin Kim CJ. Creating, Transporting, Cutting, and Merging Liquid Droplets by Electrowetting-Based Actuation for Digital Microfluidic Circuits. *J Microelectromech Syst* (2003) 12(1):70–80. doi:10.1109/JMEMS.2002.807467
6. Heikenfeld J, Smith N, Dhindsa M, Zhou K, Kilaru M, Hou L, et al. Recent Progress in Arrayed Electrowetting Optics. *Opt Photon News* (2009) 20(1):20. doi:10.1364/OPN.20.1.000020
7. Heikenfeld J, Zhou K, Kreit E, Raj B, Yang S, Sun B, et al. Electrofluidic Displays Using Young-Laplace Transposition of Brilliant Pigment Dispersions. *Nat Photon* (2009) 3(5):292–6. doi:10.1038/nphoton.2009.68
8. Van DW, and Hayes RA. *Electrowetting Elements*. U.S. Patent 8980141 (2011).
9. Ishida M, Shiga Y, Takeda U, and Kadowaki M. *Ink Containing Anthraquinone Based Dye, Dye Used in the Ink, and Display*. U.S. Patent 8999050 (2013).
10. Shiga Y, Takeda U, Ichinosawa S, and Ishida M. *Ink Containing Heterocyclic Azo Dye, and Dye for Use in Said Ink*. U.S. Patent 8747537 (2014).
11. Shiga Y, and Ishida M. *Pyrazole Disazo Dye and Ink Containing the Dye*. U.S. Patent 8143382 (2012).
12. Chiang Y, and Chao Y. Synthesis of Dis-Azo Black Dyes for Electrowetting Displays. *Mater Sci Eng B* (2012) 177(18):1672–7. doi:10.1016/j.mseb.2012.08.011
13. Farrand LD, Smith N, Corbett A, and Merck Patent GmbH L, A. *Electrowetting Fluids*. U.S. Patent 20150355456 A1 (2015).
14. Chiang Y-F, and Chao Y-C. Synthesis and Application of Oil-Soluble Red Dyes Derived from P-N-Alkyl Aniline. *Msa* (2014) 05(8):485–90. doi:10.4236/msa.2014.58052
15. Kato T, Higuchi S, Fukushige Y, Jimbo Y, and Sasaki D. *Colored Composition for Electrowetting Display, Image Display Structure, and Electrowetting Display Device*. U.S. Patent 9494789 (2014).
16. Lee PTC, Chiu C-W, Chang L-Y, Chou P-Y, Lee T-M, Chang T-Y, et al. Tailoring Pigment Dispersants with Polyisobutylene Twin-Tail Structures for Electrowetting Display Application. *ACS Appl Mater Inter* (2014) 6(16):14345–52. doi:10.1021/am503599k
17. Lee PTC, Chiu C-W, Lee T-M, Chang T-Y, Wu M-T, Cheng W-Y, et al. First Fabrication of Electrowetting Display by Using Pigment-In-Oil Driving Pixels. *ACS Appl Mater Inter* (2013) 5(13):5914–20. doi:10.1021/am401840b
18. Beni G, and Tenan MA. Dynamics of Electrowetting Displays. *J Appl Phys* (1981) 52(10):6011–5. doi:10.1063/1.329822
19. Deng Y, Jiang H, Ye D, Zhou R, Li H, Tang B, et al. Synthesis and Application of an Alkylated Pyrazole-Based Azo Dye for Electrofluidic Display. *Jnl Soc Info Display* (2018) 26(6):369–75. doi:10.1002/jsid.668
20. Baxter G, Giles CH, and Lewington WJ. Relation between Physical State and Rate of Fading of Dyes. *J Soc Dyers Colourists* (1957) 73(8):386–92. doi:10.1111/j.1478-4408.1957.tb02210.x
21. Deng Y, Li S, Ye D, Jiang H, Tang B, and Zhou G. Synthesis and a Photo-Stability Study of Organic Dyes for Electro-Fluidic Display. *Micromachines* (2020) 11(1):81. doi:10.3390/mi11010081
22. Van DW, Melanie M, Massard R, and Hayes RA. *Improvements in Relation to Electrowetting Elements*. U.S. Patent WO2010031860 A2 (2010).

Conflict of Interest: The authors declare that the research was conducted in the absence of any commercial or financial relationships that could be construed as a potential conflict of interest.

Publisher's Note: All claims expressed in this article are solely those of the authors and do not necessarily represent those of their affiliated organizations, or those of the publisher, the editors and the reviewers. Any product that may be evaluated in this article, or claim that may be made by its manufacturer, is not guaranteed or endorsed by the publisher.